CHEMIJA. 2008. Vol. 19. Nos. 3–4. P. 7–15

Pseudocapacitive behaviour of cobalt oxide films on nano-fibre and magnetron-sputtered substrates

Svetlana Lichušina,

Ala Chodosovskaja,

Algis Selskis,

Konstantinas Leinartas,

Povilas Miečinskas,

Eimutis Juzeliūnas*

Institute of Chemistry,
A. Goštauto 9,
LT-01108 Vilnius, Lithuania

Pseudocapacitance of cobalt (hydro)oxides was studied on parent substrates with different structural properties: nano-fibre structure, magnetron-sputtered and mechanically treated. The nano-fibred structure was formed electrochemically from an alkaline plating solution. The pseudocapacitive behaviour of the samples was studied by cyclic voltammetry in conjunction with the electrochemical quartz crystal nano-balance technique. (Hydro)oxide layers were formed on the substrates by anodic polarization. The layers exhibited a reversible reduction-re-oxidation behaviour with the corresponding pseudocapacitive behaviour. The nano-gravimetric measurements indicated a distinct electrode mass growth during the first anodic polarization scan, while the mass actually did not change during the reversible potential scan. The oxide layer stability was demonstrated by applying polarization cycles in the order of several thousand. The charge capacity for the nano-fibre sample was found to be up to 5 times higher as compared to a conventional cobalt surface (mechanically abraded). EQCM data have shown that the electrochemical charge transfer reactions Co(II) ↔ Co(III) ↔ Co(IV) are not associated with a remarkable electrode mass change. A novel *in-situ* approach was proposed to evaluate pseudocapacitive performance by measuring the charge value per one mass unit of oxygen (O^{2-}) within the oxide structure.

Key words: cobalt oxide, pseudocapacitance, nanostructure, EQCM, supercapacitors

INTRODUCTION

Electrochemical capacitors (or supercapacitors, ultracapacitors) are of increasing importance as a high power energy source, which could be an alternative to pulse batteries. Application of electrochemical capacitors becomes promising in such technological fields as telecommunication devices, electric and hybrid vehicles, etc. It is reasonable for many technical subjects to consider separating energy and power individually enabling to provide a peak (pulse) power at a short time. As traditional capacitors used in electronics cannot store the required energy quantity, high energy density capacitors (electrochemical capacitors) are being developed [1, 2]. The electrochemical capacitors, as compared to batteries (both pulse and conventional), are expected to have at least one order of magnitude higher power and a longer shelf and cycle life [2].

The mechanism of storage of energy by a supercapacitor involves double-layer capacitance (physical) and electrochemical pseudo-capacitance, which is due to Faradaic (charge transfer) reactions between the solids and the electrolyte. There are three main types of materials – carbon, conducting polymers and metal oxides – used to produce electrochemical capacitors. Pseudocapacitance studies of metal oxide films are of increasing importance; research groups around the world are attempting to find the performance- and cost-competitive oxides for commercial development of supercapacitors.

Ruthenium oxide has been shown to be probably the best electrode material in terms of a high specific capacitance, wide potential window and a long shelf and cycle life [2–4]. Especially the amorphous hydrated RuO_2 exhibited a high specific capacitance (over 800 F g^{-1}) [5, 6]. However, a critical issue in commercialization of the electrodes made of ruthenium oxide is the high cost of the material. For this reason, attempts to find cheaper substitutes have been undertaken. So, manganese oxide films were formed by sol-gel or electrochemical deposition with the pseudocapacitance values in the range of 50–700 F g^{-1} [7–12]. NiO_x thin films were prepared by electrochemical precipitation of $Ni(OH)_2$ and subsequent heat-treatment with the maximum specific capacitance of 277 F g^{-1} [13]. The authors extended their study to the carbon nanotube substrate on which the nickel oxide film showed a superior specific capacitance around 1000 F g^{-1} [14].

The first studies to examine cobalt oxides as an electrode material for a supercapacitor have been launched around a decade ago [15]. The authors used the electrochemical precipitation technique which yielded a rather low specific capacitance (about 40 F g^{-1}). One year later, a much higher capacitance of ca. 290 F g^{-1} was reported for cobalt oxide xerogel powders prepared by the sol–gel process by Lin et al. [16].

* Corresponding author. E-mail: ejuzel@ktl.mii.lt

Electrochemical charge transfer in cobalt oxides has been studied by Liu, Pell and Conway [17]. The authors came to a conclusion that the Co oxide film, though behaving analogously to RuO_2, has several unfavourable performance features such as limited capacitance density, rather short operable potential window and quite non-constant capacitance within the window. Nevertheless, other authors attempted to find Co oxide systems of superior performance.

Studies were carried out in the preparation of binary manganese–cobalt oxides. The oxide mixture was prepared by anodic deposition, which exhibited specific capacitance of *ca*. 125 F g^{-1} [18]. It was shown that Co addition to Mn oxide in small concentrations (0.05–0.1 M) slightly decreased the specific capacitance and inhibited the anodic dissolution of Mn [19]. Higher Co contents, however, reduced the specific capacitance significantly.

Mixtures of RhO_x with Co_3O_4 were deposited by thermal decomposition of mixtures of nitrate precursors [20]. The mixtures have been found to be good materials in terms of electrochemical capacitance (500–800 F g^{-1} at 20–60 mol. % of RhO_x).

A few research groups have recently focused on studies of the electrochemical capacitance properties of cobalt (hydro) oxides applied to nano-sized composite structures. A composite material consisting of $Co(OH)_2$ on ultra-stable Y zeolyte molecular sieves was prepared by Cao and co-workers [21]. The maximum specific capacitance 1492 F g^{-1} was obtained, which, according to the authors, was the highest one reported for supercapacitors. A mesoporous nanocrystalline Co_3O_4 was deposited from a gel–floccules system, mixing the oxide with conducting graphite and forming the composite layer onto the nickel substrate [22]. The material exhibited a specific capacitance of ca. 400 F g^{-1}. The CoOOH nano-flake films were formed on nickel by immersing the substrate into a methanol / water mixed solution of cobalt acetate with the subsequent drying at 60 °C [23]. The capacitance around 200 F g^{-1} was determined for the system. Cathodic electrodeposition of cobalt films with flower-like nanostructure was reported by Nguyen et al. [24]. The authors report a redoxable behaviour of the film during cyclic voltammetry measurements. No data, however, were given concerning the pseudocapacitive performance of the system.

Our investigation addresses an influence of the nanostructuring effect of substrate on the pseudocapacitance of electrochemically formed oxide films. Three types of materials were investigated: conventional, sputtered and of nano-fibred structure. The research focuses on searching for a relatively simple and cost-competitive method to improve the electrochemical capacitive performance of metal oxides on a parent metal.

EXPERIMENTAL

The cobalt coatings with the nano-fibre structure were deposited from the electrolyte for Zn–Co alloy electroplating as described in the patent [25], with the only difference that zinc ions were excluded from the plating bath. The electrolyte was prepared using analytical class purity reagents $CoSO_4 \cdot 7H_2O$ (20 g l^{-1}), NaOH (100 g l^{-1}), a complexing agent (40 g l^{-1}) and triply distilled water. The coatings were deposited on carbon steel plates (S = 1 cm^2) pre-treated with emery paper (grade 2500) and MgO powder, rinsed with 5% HCl and finally with distilled water.

A Parstat 2273 potentiostat from Princeton Applied Research Instruments (USA) was used to carry out cyclic voltammetry measurements. A three-electrode cell with platinum foil as a counter electrode and silver / silver chloride as a reference one were used. The solution in these measurements was 1 M NaOH, which was deoxygenated prior to measurements with Ar gas.

Electrochemical quartz crystal microbalance (EQCM) measurements were performed using the above potentiostat in conjunction with a PAR 922 microgravimetric unit from Princeton Applied Research Instruments (USA). Quartz discs with fundamental frequencies f_o = 5 MHz were used in the measurements. The oscillator is characteristic of the coefficient between the frequency and mass change K = 18 ng Hz^{-1} cm^{-2}.

A sub-layer of iron was sputtered onto quartz discs by the magnetron sputtering technique employing a magnetron sputtering system from Leybold Vacuum (Germany).

The surface structure of the deposits was studied by scanning electron microscopy (SEM) (EVO 50 EP, Carl Zeiss SMT AG, Germany) with energy dispersive and wave dispersion X-ray spectrometers (Oxford, UK).

RESULTS AND DISCUSSION

The Co electrochemical deposition characteristics were studied *in situ* by depositing the coating under EQCM control. One side of the quartz oscillator was coated with iron by the magnetron sputtering technique. Figure 1 provides data on mass and potential change during galvanostatic deposition of cobalt. The rectilinear mass growth from the very beginning till ca. 1.5 h indicated a constant deposition rate, while during a longer electrolysis time the rate tended slightly to decrease. The current efficiency derived from the mass change rate according to Faraday's law was approximately 50%.

SEM images in Fig. 2 (a, b, c) show the surface topography of the deposits on a sub-micrometre scale. The pristine electrochemically deposited structure (a) consists of randomly distributed nano-fibres with the thickness in the order of tens of nanometres and the length in the order of hundreds of nanometres. A similar structure was obtained both on the carbon steel substrate and on the sputtered iron (Figs. 2 and 3). The sputtered specimen, both pristine (Fig. 4a) and oxidized (Fig. 4b), differed markedly in their surface morphology. During a prolonged cycling, the fibre structure is transformed into flower-like one (Fig. 2b), whereas oblong pits are observed for the sputtered specimen (Fig. 4b). Figure 5 gives the microtopography of mechanically treated sample for comparison.

EQCM data obtained for an electrochemically deposited cobalt sample during a prolonged exposure at the open circuit potential (E_{ocp}) in 1 M NaOH are shown in Fig. 6. (Similar results were obtained for a sputtered sample as well; the data are not provided in the paper.) The electrode mass rapidly increased after immersion during some 15 min at the rate dm/dt ≈ 0.25 μg cm^{-2} s^{-1}. The mass increase was accompanied by a negative shift

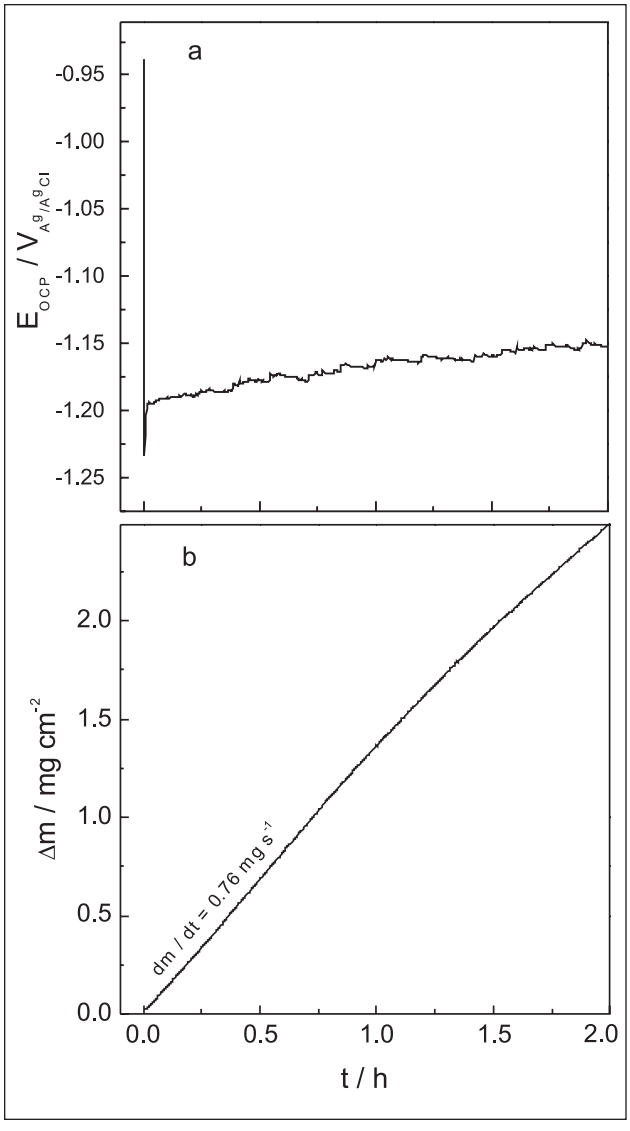

Fig. 1. Potential and mass change during galvanostatic deposition of cobalt at i_c = mA cm^{-2} determined by EQCM

of E_{ocp}. The process may be attributed to cobalt (hydro)oxide formation on the electrode surface [26]:

$$Co + 2OH^- \rightarrow Co(OH)_2 + 2e^- \quad (1)$$

$$Co + 2OH^- \rightarrow CoO + H_2O + 2e^- \quad (2)$$

with standard potentials at pH 14 E_o = –0.918 $V_{Ag/AgCl}$ and E_o = –0.892 $V_{Ag/AgCl}$, respectively. After some time, the oxide layer reached its maximum thickness, and its slight dissolution became prevailing over the deposition process. The dissolution may be assumed according to Pourbaix diagrams to proceed as follows:

$$CoO + H_2O \rightarrow HCoO_2^- + H^+. \quad (3)$$

The dissolution process is clearly indicated by the presence of maximum on the mass curve in Fig. 3. Some instabilities in mass change observed at final stages of exposure indicate a competition between the processes of deposition and dissolution.

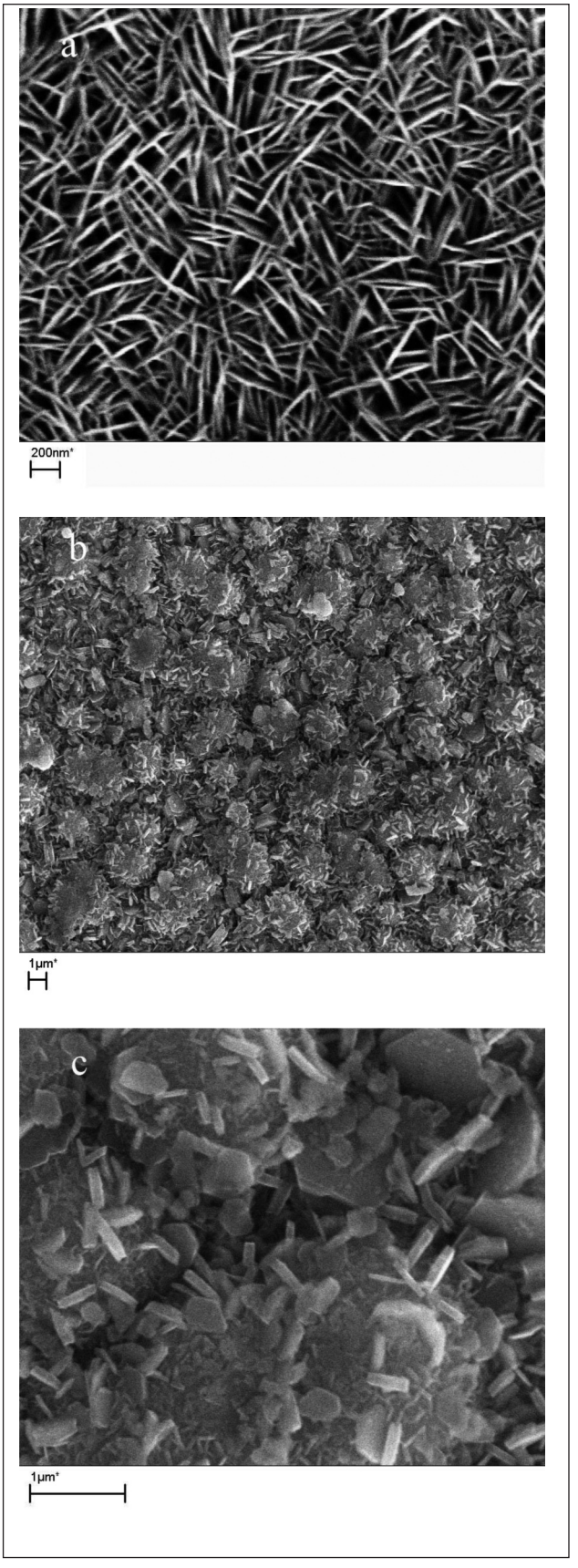

Fig. 2. SEM images of electrochemically formed nano-fibre structure of Co on carbon steel substrate: a – pristine surface; b and c – after 1820 polarization cycles in 1 M NaOH at different magnifications

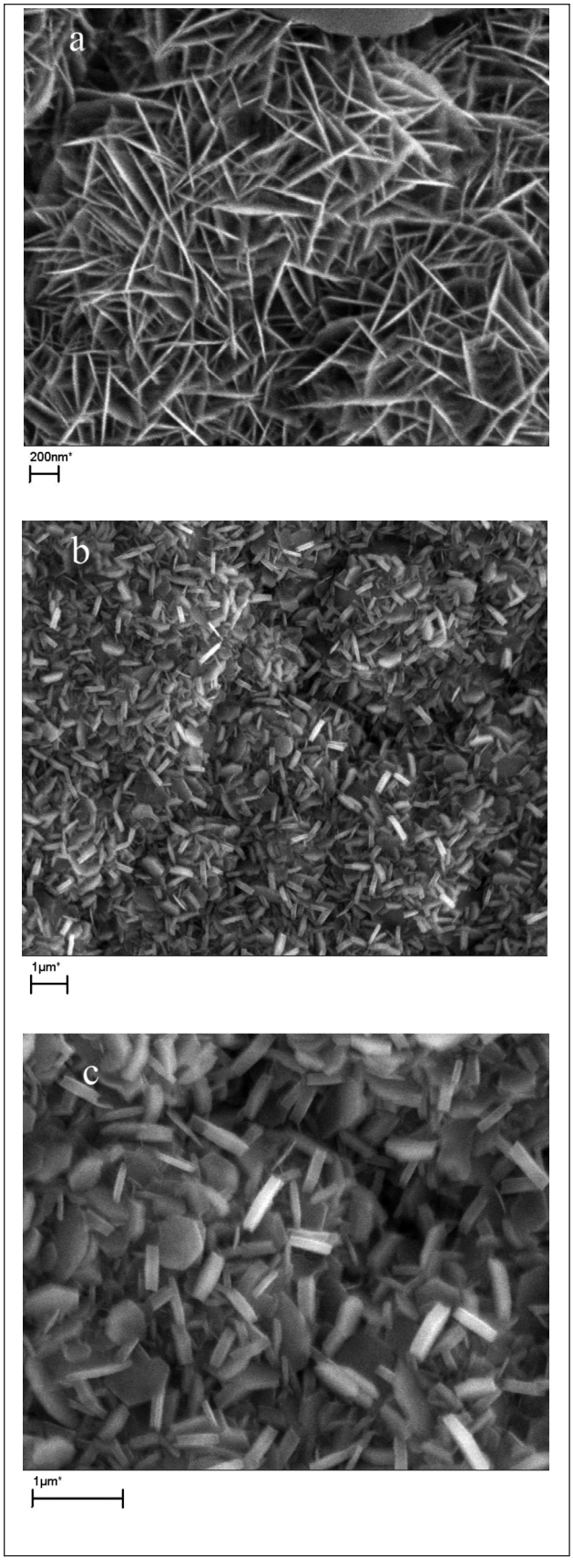

Fig. 3. SEM images of electrochemically formed nano-fibre structure of Co on magnetron sputtered iron coating: a – pristine surface; b and c – after 110 polarization cycles in 1 M NaOH at different magnifications

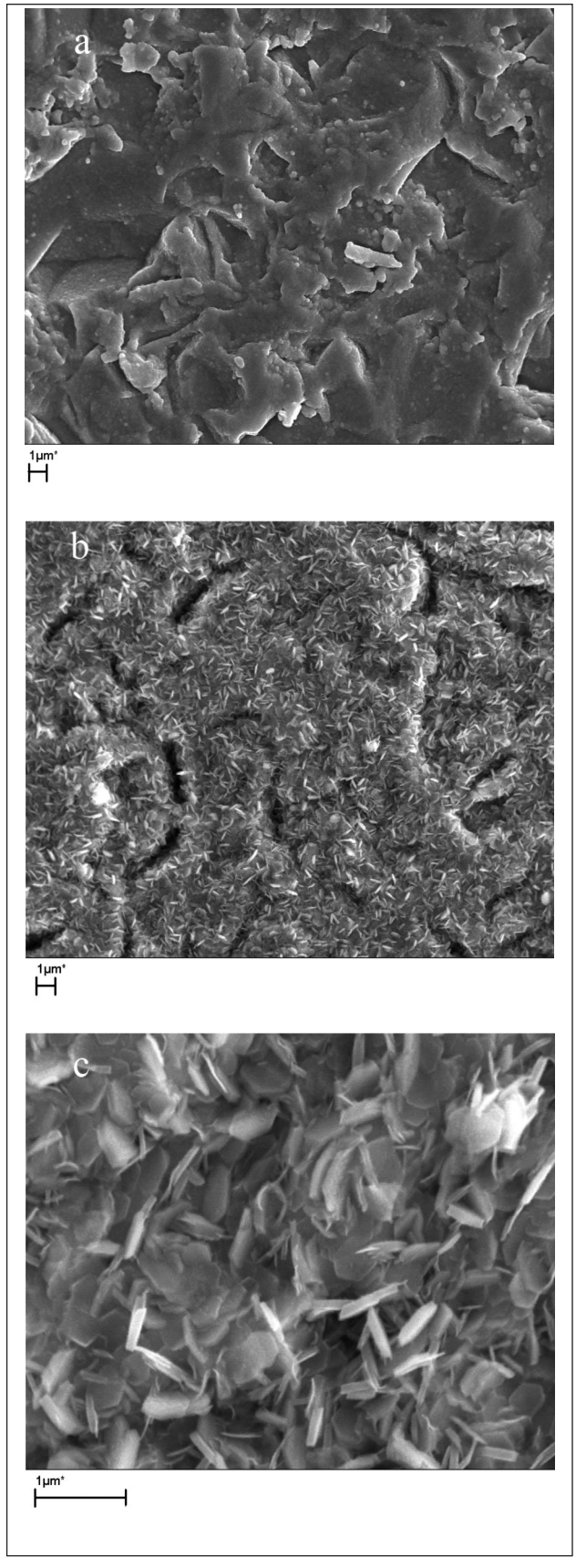

Fig. 4. SEM images of magnetron sputtered Co on quartz (a) and the oxide surfaces after 100 polarization cycles (b, c) in 1 M NaOH at different magnifications

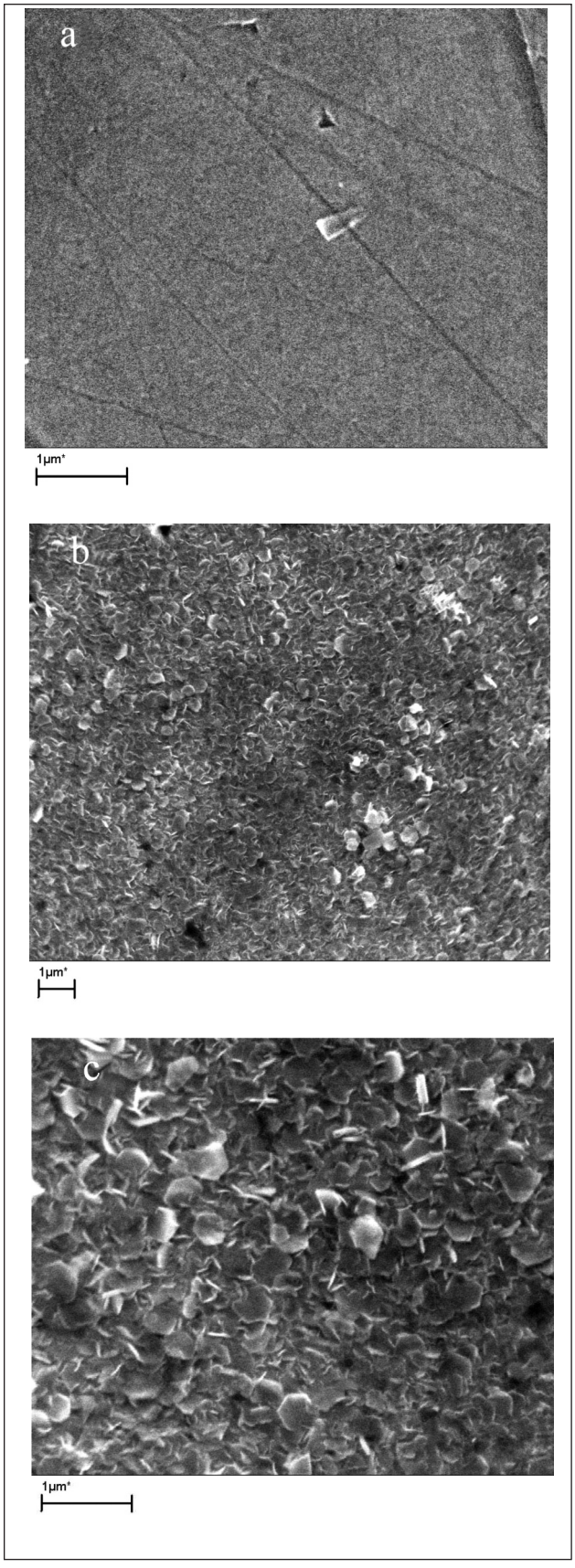

Fig. 5. SEM images of mechanically treated Co surface (a) and the oxide surfaces after 100 polarization cycles (b, c) in 1 M NaOH at different magnifications

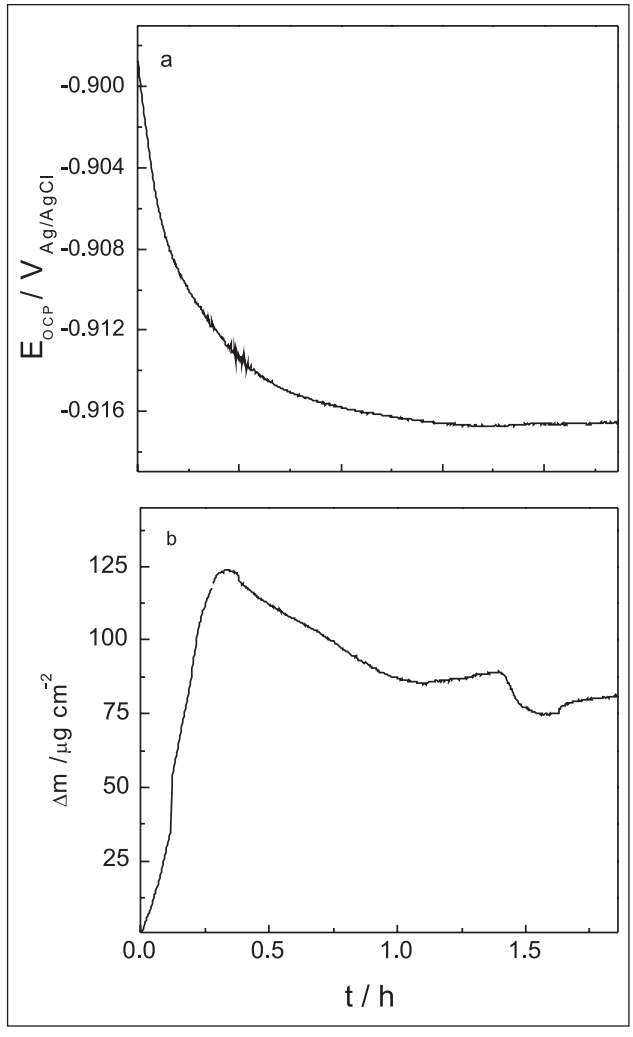

Fig. 6. Change of open circuit potential and electrode mass during prolonged exposure of cobalt electrode to 1 M NaOH

Cyclic voltammetry experiments (Fig. 7) revealed a highly irreversible anodic-cathodic behaviour of the electrode during the first several cycles. A large anodic peak was observed during the first cycle, which gradually decreased during the subsequent cycling. The system was getting increasingly reversible with the cycling, as is evident from the curves for cycles 7–10 in Fig. 7 and prolonged cycling in Fig. 8.

The magnitude of the first current peak clearly depends on the structural-morphological properties of the surfaces (Fig. 9). The quantity of the electricity increases markedly in the following sequence: conventional cobalt, sputtered sample, nano-fibre structure. The peak is attributed to surface oxidizing according to reactions 1 and 2. Data in Fig. 9 clearly imply that the greatest amount of the oxide is formed on the nano-fibred structure.

Figure 8 compares the cathodic and anodic branches of the voltammograms after a prolonged cycling. The current responses increase during the cycling as indicated by the curves for the 11th and the 330th cycle. The coincidence of the curves during prolonged cycling (e. g. those for the 330 and 1000 cycles) indicates a high cycle life of the oxide layer. This property is important for the practical application of the system in supercapacitors.

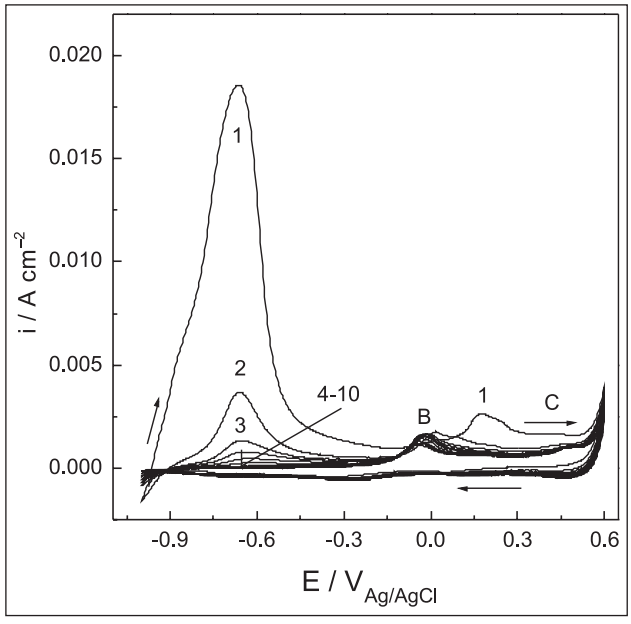

Fig. 7. Cyclic voltammetry curves (ten cycles) for electrochemically deposited cobalt on steel substrate in 1 M NaOH at potential scan rate 20 mV s^{-1}

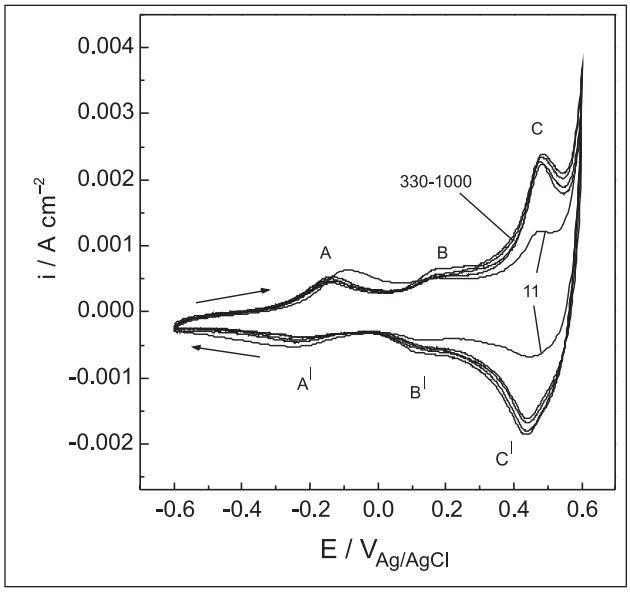

Fig. 8. Subsequent cycling of the electrode up to 1000 cycles following the measurements shown in Fig. 7

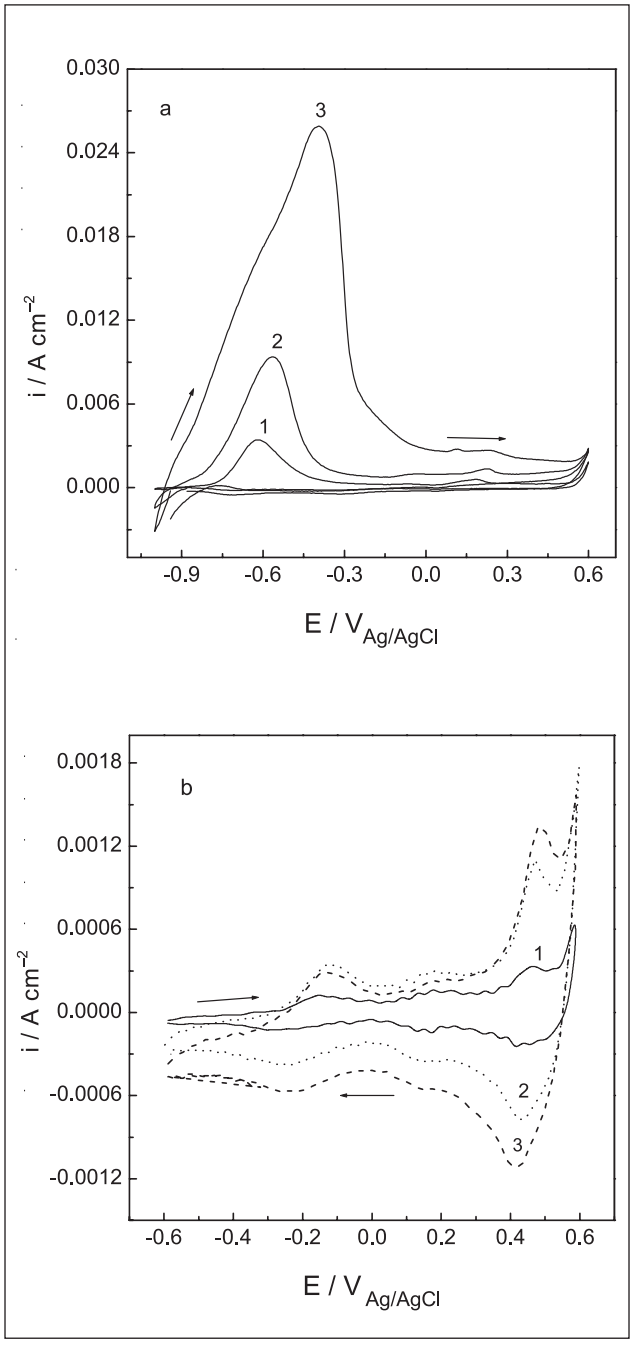

Fig. 9. First polarization cycle (a) and after 100 cycles (b) for conventional Co – 1, sputtered sample – 2 and nano-fibre structure – 3

Three distinctive peaks in Fig. 8 (A, B and C) indicate the main electrochemical transformations of the oxide layer during potential scan. According to the Pourbaix diagrams, the cobalt oxidation states are Co^{2+}, Co^{3+} and Co^{4+}, which may form $Co(OH)_2$, $HCoO^{2-}$, Co_3O_4, $Co(OH)_3$ and CoO_2. The location of the three peaks in the diagram may be attributed to the following reactions:

$$(A)\ 3Co(OH)_2 + 2OH^- \rightarrow Co_3O_4 + H_2O + 2e^-, (E_0 = -0.292\ V_{Ag/AgCl}) \quad (4)$$

$$CoO + OH^- \rightarrow CoOOH + e^-\ (E_o = -0.272\ V_{Ag/AgCl}), \quad (5)$$

$$(B)\ Co_3O_4 + OH^- + H_2O \rightarrow 3CoOOH + e^-\ (E_o = 0.122\ V_{Ag/AgCl}), \quad (6)$$

$$(C)\ CoOOH + OH^- \rightarrow CoO_2 + H_2O + e^-\ (E_o = 0.462\ V_{Ag/AgCl}). \quad (7)$$

The anodic and cathodic charge quantities that passed during the polarization cycles are summarized in Table. The obtained values for the nano-structured sample are up to five times higher than those determined for a conventional (mechanically abraded) cobalt surface. For instance, the charge value for conventional cobalt was Q_a = 7.1 mC cm^{-2} at the cycle number 120, whereas the analogous value for the nanostructure is about

Table. **Anodic and cathodic charges passed during the potential scan cycles for Co in 1 M NaOH and the difference between the anodic and cathodic charge values. Potential scan rate – 20 mV s^{-1}**

Cycle number	Q_a, mC cm^{-2}	Q_c, mC cm^{-2}	Q_a–Q_c, mC cm^{-2}
11	33.8	36.2	–2.4
330	34.9	31.0	3.9
530	34.4	31.7	2.7
730	37.0	33.2	4.2
930	38.5	35.7	2.8
1620	42.2	45.8	3.6
1800	43.4	52.4	9.0

five times higher (Q_a = 34 mC cm^{-2}). Also, the analogous data for cobalt referred to in the literature [17] are about four times lower as compared to the nano-fibre structure. The data clearly show the enhancing effect of surface nanostructuring on electrochemical capacity.

EQCM measurements indicate the distinctive mass effects which occur during the cyclic polarization of the cobalt electrode (Figs. 10 and 11). A large anodic current response observed during the first polarization scan yields an exponential mass growth with a subsequent wide potential range of constant mass behaviour (ca. –0.3 V–0.6 V). When reversing the potential scan, an irreversible current is observed with no remarkable mass effects over a wide potential range (some mass growth is observed only below ca. 0.7 V). The total mass gain

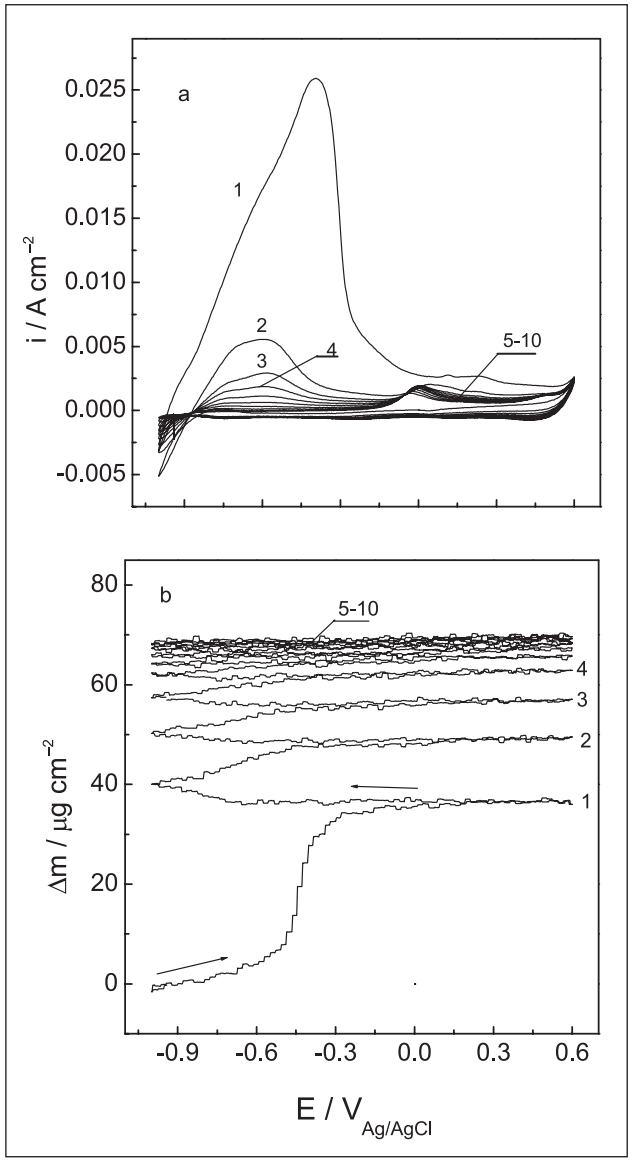

Fig. 10. EQCM and cyclic voltammetry data for electrochemically deposited cobalt in 1 M NaOH. Potential scan rate 20 mV s^{-1}

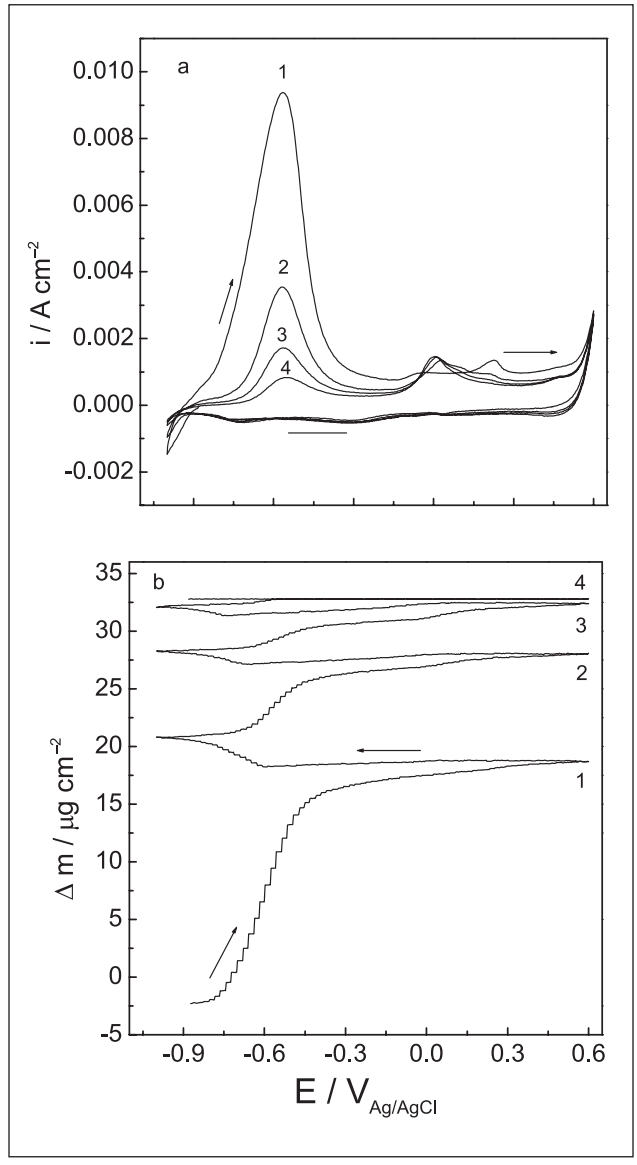

Fig. 11. EQCM and cyclic voltammetry data for magnetron sputtered cobalt in 1 M NaOH. Potential scan rate 20 mV s^{-1}

decreases gradually during the subsequent potential scans approaching some limiting value, which was determined to be $\Delta m \approx 75$ μg cm^{-2} for electrochemically deposited specimen and $\Delta m \approx 44$ μg cm^{-2} for the sputtered sample (after 100 polarization cycles).

The EQCM data confirm that the oxide is produced only around the first large current peak (Fig. 7). The subsequent peaks (A, B and C, Fig. 8) do not impose significant mass effects. The currents are associated with charge transfer phenomena within the oxide structure without changing its total mass, as predicted by equations 4–7.

The entire increase in the electrode mass after the 10th cycle is $\Delta m \approx 69$ μg cm^{-2} (Fig. 10). The mass growth can be supposed to be caused predominantly by oxygen (O^{2-}) attachment to the surface when assuming the anodic CoO or $Co(OH)_2$ generation. From the oxygen mass we can calculate the mass of the produced oxide to be $m_{CoO} = 323$ μg cm^{-2}. The anodic charge that passed during the 10th polarization cycle was determined to be $Q_a = 0.033$ C cm^{-2} and the potential window $\Delta E \approx -0.83$ V, which gives the capacity value $C = 123$ F g^{-1}. The analogous calculation assuming $Co(OH)_2$ gives $C = 218$ F g^{-1}. These values approximate the lower and upper limits of the capacitance to be expected per one gram of the (hydro)oxide weighed *in situ*. It should be stressed that the provided values are not straightforwardly comparable with the numerous super-capacitance values in the literature [2–24], which relates to the oxides weighed under *ex-situ* conditions.

Due to the ambiguity in the chemical composition of the surface layer, it seems reasonable to express the pseudocapacitance value per oxygen unit whose determination by EQCM does not seem problematic. So, for the 10th cycle discussed above, the oxygen mass on the electrode is $\Delta m \approx 69$ μg cm^{-2}, and the corresponding capacitance value will be 576 F per one gram of the attached oxygen.

As a concluding remark, it should be noted that, although the surface nano-structuring enhances the cobalt oxide capacity several times, its performance in the view of the best examples reported in the literature looks moderate. From the practical point of view, however, the system under study is rather interesting, because the proposed electrochemical method of electrode preparation looks commercially attractive because of its cost-effectiveness and technical simplicity.

CONCLUSIONS

The pseudocapacitance of cobalt (hydro)oxides was studied on nano-fibre structure which was formed electrochemically from an alkaline plating solution. The (hydro)oxide structure formed on the substrate by anodic polarization exhibited reversible reduction-reoxidation with the corresponding pseudocapacitive behaviour. The layer stability has been demonstrated by applying polarization cycles in the order of several thousands.

The charges passed in the polarization cycles for the nano-fibre sample were found to be up to five times higher as compared to those determined for a conventional (mechanically abraded) cobalt surface and up to four times *versus* those reported in the literature.

A distinct electrode mass growth was identified by nano-gravimetric measurements during the first anodic polarization scan, while the mass actually did not change during the reversible potential scan. The data have confirmed that oxide formation occurs mainly during the initial polarization.

The electrochemical capacity was due to electrochemical charge transfer reactions Co(II) ↔ Co(III) ↔ Co(IV) which according to EQCM data are not associated with remarkable electrode mass changes.

A novel approach has been proposed to evaluate pseudocapacitance performance *in situ* by measuring the charge value per oxygen mass unit within the oxide structure.

Received 1 October 2008
Accepted 15 October 2008

References

1. B. E. Conway. *Electrochemical Capacitors: Scientific Fundamentals and Technological Applications*, Kluwer Academic / Plenum (1999).
2. A. Burke, *J. Power Sources*, **91**, 37 (2000).
3. J. P. Zheng, P. J. Cygan, T. R. Jow, *J. Electrochem. Soc.*, **142**, 2699 (1995).
4. Z. Chen, S. A. Merryman, *Proceedings of the 9th International Seminar on Double-layer Capacitors and Similar Energy Storage Devices, Deerfield Beach, FL, December* (1999).
5. W. Sugimoto, H. Iwata, Y. Yasunaga, Y. Murakami, Y. Takasu. *Angew. Chem. Int. Ed.*, **42**, 4092 (2003).
6. M. Hughes, G. Z. Chen, M. S. P. Shaffer, D. J. Fray, A. H. Windle, *Chem. Mater.,* **14**, 1610 (2002).
7. H. Y. Lee, J. B. Goodenough, *J. Solid State Chem*., **144**, 220 (1999).
8. S. C. Pang, M. A. Anderson, T. W. Chapman, *J. Electrochem. Soc.,* **147**, 444 (2000).
9. C.-C. Hu, T.-W. Tsou, *Electrochem. Commun*., **4**, 105 (2002).
10. J. Jiang, A. Kucernak, *Electrochim. Acta,* **47**, 238 (2002).
11. Y. U. Jeong, A. Manthiram, *J. Electrochem. Soc.,* **149**, A1419 (2002).
12. J.-K. Chang, W.-T. Tsai, *J. Electrochem. Soc.,* **150**, A1333 (2003).
13. K.-W. Nam, K.-B. Kim, *J. Electrochem. Soc.*, **149**, A346 (2002).
14. K.-W. Nam, E.-S. Lee, J.-H. Kim, Y.-H. Lee, K.-B. Kim, *J. Electrochem. Soc.,* **152**, A2123 (2005).
15. V. Srinivasan, J. W. Weidner, *J. Electrochem. Soc.*, **144**, L210 (1997).
16. C. Lin, J. A. Ritter, B. N. Popov, *J. Electrochem. Soc.*, **145**, 4097 (1998).
17. T.-C. Liu, W. G. Pell, B. E. Conway, *Electrochim. Acta*, **44**, 2829 (1999).
18. P.-Y. Chuang, C.-C. Hu, *Materials Chemistry and Physics,* **92**, 138 (2005).
19. J.-K. Chang, M.-T. Lee, C.-H. Huang. W.-T. Tsai, *Materials Chemistry and Physics*, **108**, 124 (2008).
20. A. R. Souza, E. Arashiro, H. Golveia, T. A. F. Lassali, *Electrochim. Acta*, **49**, 2015 (2004).
21. L. Cao, F. Xu, Y.-Y. Liang, H. L. Li, *Adv. Mater.*, **16**, 1853 (2004).

22. L. Cao, M. Lu, H.-L. Li, *J. Electrochem. Soc*., **152**, A871 (2005).
23. E. Hosono, S. Fujihara, I. Honma, M. Ichihara, H. Zhou, *J. Power Sources*, **158**, 779 (2006).
24. Q. Nguyen, L. Wang, G. M. Lu, *Int. J. Nanotechnol.*, **4**, 588 (2007).
25. E. Juzeliunas, S. Lichusina, Patent of the Republic of Lithuania, No. 5481 (2008).
26. W. K. Behl, J. E. Toni, *J. Electroanal. Chem*., **31**, 63 (1971).

Svetlana Lichušina, Ala Chodosovskaja, Algis Selskis, Konstantinas Leinartas, Povilas Miečinskas, Eimutis Juzeliūnas

PSEUDOTALPUMINĖ KOBALTO OKSIDO PLĖVELIŲ, SUFORMUOTŲ ANT KOBALTO NANOSIŪLELIŲ IR UŽDULKINTŲ MAGNETRONIŠKAI, ELGSENA

S a n t r a u k a

Ištirta pseudotalpa kobalto (hidro)oksidų, suformuotų ant skirtingų struktūrų substrato: nanosiūlelių, magnetroniškai uždulkinto ir mechaniškai apdoroto. Co nanosiūleliai buvo suformuoti elektrochemiškai šarminiame tirpale. Pseudotalpuminė kobalto oksidų elgsena buvo ištirta ciklinės voltamperometrijos metodu panaudojant elektrocheminės kvarco kristalo svarstykles (EKKM). Anodinės poliarizacijos būdu ant įvairių substratų buvo suformuoti kobalto (hidro)oksido sluoksniai. Oksidiniai sluoksniai parodė grįžtamą redukcijos–reoksidacijos ir atitinkamą pseudotalpuminę elgseną. Nanogravimetriniai matavimai parodė būdingą elektrodo masės augimą per pirmąjį anodinį potencialo skleidimą ir praktiškai nekintančią masę per grįžtamąjį potencialo skleidimą. Per kelis tūkstančius anodinių ciklų buvo parodyta, kad oksidinis sluoksnis išliko stabilus. Nustatyta, kad oksidų, suformuotų ant elektrodo su nanosiūlelių struktūra talpa maždaug 5 kartus didesnė nei oksidų ant mechaniškai poliruoto Co. EKKM duomenys parodė, kad elektrocheminės Co(II) ↔ Co(III) ↔ Co(IV) reakcijos nėra susijusios su žymiais elektrodo masės pokyčiais. Buvo pasiūlytas naujas būdas įvertinti pseudotalpuminę elgseną – krūvis, tenkantis vienam deguonies (O^{2-}) masės vienetui oksido struktūroje.